

Permanent narrow-band reflection holograms for infrared light recorded in LiNbO₃:Ti:Cu channel waveguides

J. Hukriede, D. Kip, E. Krätzig

Universität Osnabrück, Fachbereich Physik, 49069 Osnabrück, Germany
 (Fax: +49-541/969-3510, E-mail: joerg.hukriede@uos.de)

Received: 2 October 2000/Revised version: 25 January 2001/Published online: 22 March 2001 – © Springer-Verlag 2001

Abstract. Permanent refractive-index gratings are generated by thermal fixing of holograms in photorefractive lithium niobate channel waveguides. The guides are fabricated by successive indiffusion of titanium stripes and thin layers of copper. After high-temperature recording with green light, refractive-index modulations exceeding $\Delta n = 8 \times 10^{-5}$ for light of the telecommunication wavelength 1550 nm appear without the need of any development process of the written holograms. The gratings are stable in the dark and no compensation mechanism via dark conductivity is observed. Thus this method may be well suited for long-time applications in holography and integrated optics.

PACS: 42.40.E; 42.82.E; 84.40.U

Lithium niobate (LiNbO₃) is a widely used substrate material for integrated optics due to its outstanding acousto- and electrooptical properties. Iron- or copper-doped LiNbO₃ crystals also show a pronounced photorefractive effect [1]. Both dopants appear in two valence states, Fe²⁺ (Cu⁺) and Fe³⁺ (Cu²⁺) [2]. By illumination with a light-intensity pattern, electrons are redistributed between these filled and empty traps. A space-charge field builds up that modulates the refractive index via the electrooptic effect. A common method to stabilize the recorded holograms versus the readout light is the process of thermal fixing [3,4]. Thermal fixing has been investigated intensively in iron-doped LiNbO₃ volume crystals. By this technique devices like volume narrow-band wavelength filters [5, 6] or integrated DBR (Distributed Bragg Reflector) waveguide lasers [7] for 1550 nm have been fabricated. However, devices utilizing fixed gratings in LiNbO₃:Fe suffer from a compensation process of the developed space-charge field that results from the non-negligible dark conductivity of the material: to preserve their properties they have to be periodically refreshed by a homogeneous development process with photoactive light. This is a crucial disadvantage for applications that are designed to work permanently for many years. In this contribution we investigate the technique of thermal fixing in copper-doped LiNbO₃ channel waveguides fabricated by titanium indiffusion. These guides

show photorefractive properties which are similar to those of LiNbO₃:Cu volume crystals, doped either conventionally in the melt or by indiffusion [8,9]. In our fixing experiments we find that refractive-index gratings with a refractive-index modulation exceeding $\Delta n = 8 \times 10^{-5}$ at 1550 nm can be stored permanently in the channels without the occurrence of a compensation process. This behaviour is different to the well-investigated fixing process in LiNbO₃:Fe and of significant importance for future applications.

1 Evaluation and experimental details

To diffract light from a thick refractive-index grating the Bragg condition has to be matched. The diffraction efficiency η of the grating is given by $\eta = I_d / (I_t + I_d)$, where I_t and I_d are the intensities of the transmitted and the diffracted beams, respectively. For a reflection grating, η and the refractive-index modulation Δn are related via $\eta = \tanh^2(\pi \Delta n d \lambda^{-1})$, where d is the length of the grating and λ is the Bragg wavelength [10].

For sample preparation, pieces of $8 \times 16 \text{ mm}^2$ are cut from an undoped y-cut LiNbO₃ wafer of congruently melting composition. The c-axis points along the larger side. By evaporation and additional photolithographic structuring 8- μm -wide titanium stripes of 100-nm thickness are created parallel to the c-axis on the top face of the samples. They are indiffused for 22 h in air at a temperature of 1000 °C. This forms single-mode channel waveguides for infrared light around 1550 nm. In the next step the top faces of the samples are coated with thin copper layers of various thicknesses. To increase the photorefractive effect in the channels these layers are indiffused at 1000 °C, too. The diffusion time is 2 h, long enough to ensure a practically constant copper concentration in the channels [11]. We calculate a copper-doping level of $c_{\text{Cu}} = (5.7/4.7/3.2/2.2/2.2) \times 10^{25} \text{ m}^{-3}$ in the channels for the five investigated samples (T4/S5/S3/K5/W3). The copper indiffusion is performed in wet, reducing argon atmosphere, with the exception of the sample W3 which is annealed in dry oxygen atmosphere. In a reducing environment the number of filled traps Cu⁺ is enhanced. On the other

hand the number of empty traps Cu^{2+} is enlarged by an oxidising treatment. Finally the end faces of all waveguides are precisely polished and anti-reflection-coated for the infrared readout light. The bottom face of each sample is also anti-reflection-coated for the green recording light.

Reflection gratings are recorded by interference of two coherent, ordinarily polarized plane waves of an argon-ion laser at 514.5 nm. The beams impinge upon the waveguides in the yz -plane and illuminate the whole top face. The vector \mathbf{K} of the generated interference pattern is directed along the c -axis, parallel to the channels. The light intensity is about 1200 Wm^{-2} and the recording angle is 93.87° in air. An active phase stabilization for the recording light is utilized [12]. Fixing during recording is performed by heating the waveguide to 180°C while the grating is written. After recording the samples are kept in the dark and cooled down to 20°C within 5 min.

For readout of the recorded refractive-index gratings a DFB (Distributed Feedback) laser, tunable between $\lambda = 1555.36 \text{ nm}$ and 1559.36 nm in steps of 0.01 nm , is applied. The light is guided through an optical single-mode fibre directly into the channels via end-face coupling. The light polarization is adjusted to excite the TM mode. The transmitted light is directed onto a germanium photodetector with the help of a second fibre. The recorded gratings are read by taking transmission spectra of the channels: the DFB laser is tuned and the normalized transmitted signal intensity $T(\lambda)$ is measured as a function of wavelength. When the readout wavelength matches the Bragg condition a pronounced intensity drop appears. The diffraction efficiency η is deduced from the relation $\eta = 1 - T_{\min}$, where T_{\min} is the minimal transmission at the Bragg wavelength.

After the recording process the fixed gratings are homogeneously illuminated with an expanded beam of the argon-ion laser which hits the samples perpendicular to the top face. The light intensity is about 250 Wm^{-2} . During illumination the evolution of η is measured by taking transmission spectra with the DFB laser. The dark compensation of a developed grating is monitored by taking transmission spectra while the sample is kept in the dark. The weak infrared readout light (power about $100 \mu\text{W}$) does not affect the time evolution of η . Further details regarding the waveguide fabrication and the recording and readout setup may be found in [8].

2 Experimental results

First, a reflection grating is recorded for 60 min at 180°C in the oxidised waveguide W3. After cooling down to room temperature, a transmission spectrum $T(\lambda)$ of the $8\text{-}\mu\text{m}$ -wide channel is taken. The result is shown in the upper part of Fig. 1. At this stage, only a very small Bragg peak is estimated. This is the well-expected behaviour from the theory of thermal fixing in doped LiNbO_3 volume crystals [13–15]. Then the fixed hologram is developed by illumination with green light until saturation occurs. The resulting transmission curve $T(\lambda)$ is shown in the bottom part of Fig. 1. As expected, a strong Bragg peak appears. From the measured diffraction efficiency of $\eta = 98.5\%$ for the infrared light we calculate a refractive-index modulation of $\Delta n = 1.2 \times 10^{-4}$ in the channel.

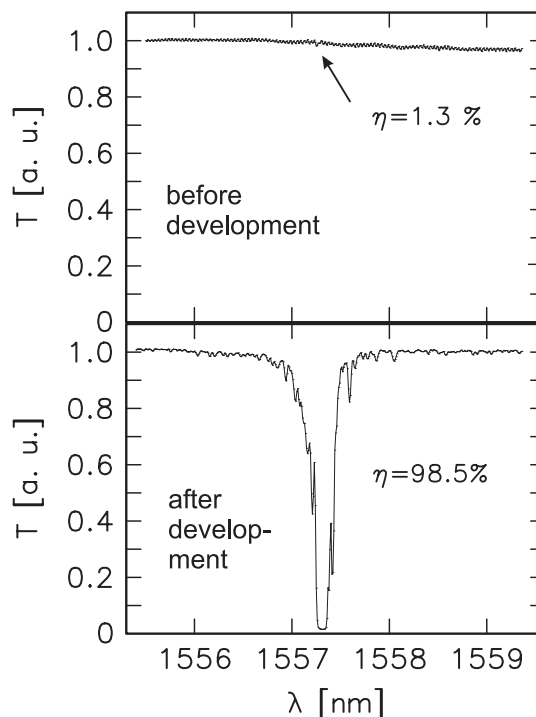


Fig. 1. Transmission T before and after the development process versus readout wavelength λ for a grating recorded for 60 min in the oxidised waveguide W3

Now we proceed with the waveguide T4. In contrast to the sample W3, this guide was annealed in reducing argon atmosphere. Furthermore, the copper concentration is more than two times higher. A grating is recorded for 120 min at 180°C . Directly after cooling down, a transmission spectrum is taken. Figure 2 shows the result for the $8\text{-}\mu\text{m}$ -wide channel. A strong peak is identified and the measured diffraction efficiency reaches 96% at a centre wavelength of $\lambda = 1557.81 \text{ nm}$. The line width (FWHM) of the fixed hologram is less than 0.09 nm . We want to emphasize that until now no development process has been applied to the sample.

In the next step the fixed grating in the sample T4 is developed with green light. The measured time evolution of the refractive-index modulation Δn is presented in Fig. 3. The value Δn first rapidly drops down, then passes through a min-

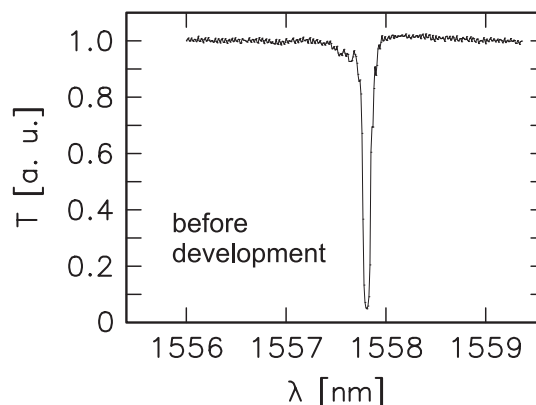


Fig. 2. Transmission T versus readout wavelength λ for a grating recorded for 120 min in the reduced waveguide T4 before the development process

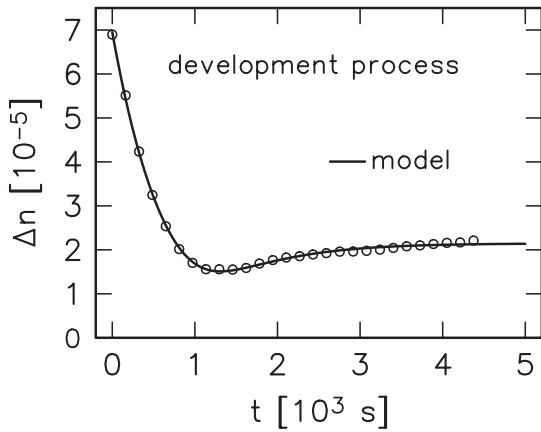


Fig. 3. Time evolution of the refractive-index modulation Δn during the development of the fixed grating in waveguide T4. The *solid line* is a fit according to (1)

imum and finally reaches a steady state after 5000 s. The final value is smaller than the initial value Δn_0 . The solid line is a fitted curve following a simple model presented in Sect. 3. This behaviour is exactly the opposite of what is expected from the common theory of thermal fixing.

Now the developed refractive-index grating is kept at room temperature in the dark and the time evolution of Δn is monitored over a total range of 250 h. The result is shown in Fig. 4. Again Δn first decreases, passes through a minimum and grows again before it finally saturates. Now the saturation value is larger than the start value. The solid line is again a fitted curve according to the model presented below. It is remarkable that the start and end values practically coincide with those obtained from the development process. This means that in the dark Δn evolves back to its initial value before the development process. In the dark the initial values Δn_0 are stable: an undeveloped grating with $\eta = 90\%$ recorded in the sample S5 shows no measurable decrease of its diffraction efficiency for a duration of more than one year.

The presented time evolution of Δn under homogeneous illumination and in the dark is similar for all four reduced waveguides investigated in this contribution: directly after recording a pronounced refractive-index modulation is al-

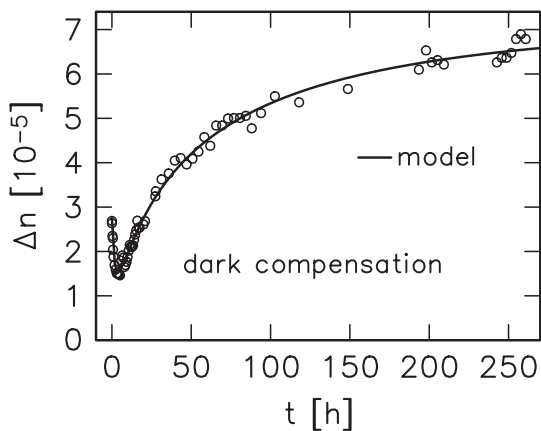


Fig. 4. Time evolution of the refractive-index modulation Δn in the dark for the grating in waveguide T4. The *solid line* is a fit according to (2)

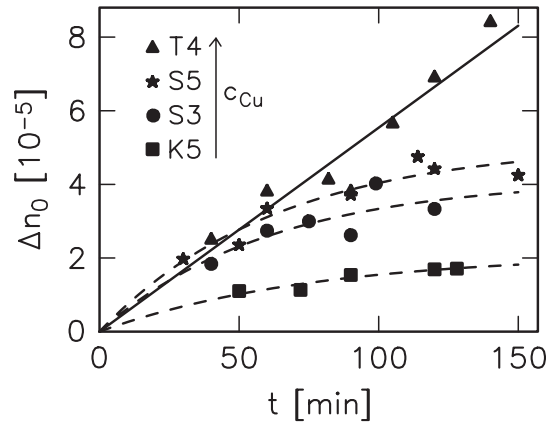


Fig. 5. Permanent refractive-index modulations Δn_0 obtained without development versus recording time t for the investigated reduced channel waveguides. The *lines* are guides for the eye

Table 1. Summary of the obtained results. The sample U3 is undoped. The copper indiffusion into the waveguides K5, S3, S5 and T4 was performed for 2 h at 1000 °C in wet argon atmosphere. For the sample W3 it was performed for 2 h at 1000 °C in dry oxygen atmosphere. c_{Cu} : copper concentration in the channels, Δn_0^{\max} : maximum of the obtained permanent refractive-index change without development, $\alpha_{1550 \text{ nm}}$: waveguide losses for the TM mode at 1550 nm

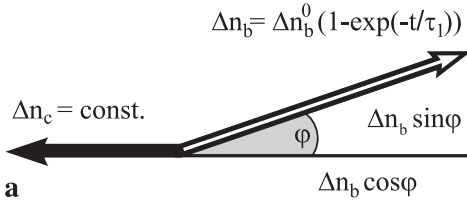
Sample	c_{Cu} [10^{25} m^{-3}]	Δn_0^{\max} [10^{-5}]	$\alpha_{1550 \text{ nm}}$ [dB cm^{-1}]
U3	–	–	0.08
K5	2.2	1.7	1.65
S3	3.2	4.0	1.98
S5	4.7	4.8	2.29
T4	5.7	8.4	2.30
W3	2.2	0.3	2.29

ready present in the channels. In the dark a developed grating tends to restore its initial value that is measured before the development process. Figure 5 shows the initial refractive-index modulations Δn_0 for the investigated reduced waveguides versus the recording time t . The values grow with the recording time and with the copper concentration in the channels. The data for the samples K5, S3 and S5 are well fitted by single exponentials with a time constant around 60 min (dashed and dotted lines in Fig. 5). The values obtained for the sample T4 still grow almost linearly in the investigated time interval (solid line). The maximum values Δn_0^{\max} , together with the copper concentrations in the channels and the measured waveguide losses at 1550 nm, are summarized in Table 1.

3 Model

To explain the observed time evolution of Δn in the reduced samples under homogeneous illumination and in the dark we assume that the measured Δn results from a superposition of two different refractive-index gratings present in the waveguides. The corresponding model is illustrated in Fig. 6. The first grating is labelled Δn_c . It grows during high-temperature recording and remains constant after cooling down. At room temperature it is not affected by photoactive light anymore. The second grating Δn_b is just generated during the development process. While the sample is illu-

development



dark compensation

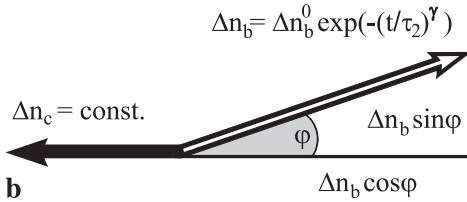


Fig. 6. Model for the refractive-index evolution during the development process and in the dark (see text)

minated homogeneously it exponentially grows with a time constant τ_1 until it saturates. The gratings have a phase difference between each other. This is indicated by the angle φ in Fig. 6.

From this model we obtain a time evolution for the development process:

$$\Delta n(t) = \sqrt{[\Delta n_c - \Delta n_b^0 \cos \varphi (1 - \exp(-t/\tau_1))]^2 + [\Delta n_b^0 \sin \varphi (1 - \exp(-t/\tau_1))]^2} \quad (1)$$

The solid line in Fig. 3 is the corresponding fit to the measured data. It yields $\Delta n_c = 7.0 \times 10^{-5}$, $\Delta n_b^0 = 8.3 \times 10^{-5}$, $\varphi = 12.6^\circ$ and $\tau_1 = 770$ s.

To describe the dark evolution of Δn after the development process we assume that the grating Δn_b is erased according to a stretched exponential function, whereas the grating Δn_c remains constant. Following the diagram in the lower part of Fig. 6 our model predicts the time evolution in the dark:

$$\Delta n(t) = \sqrt{[\Delta n_c - \Delta n_b^0 \cos \varphi \exp(-(t/\tau_2)^\gamma)]^2 + [\Delta n_b^0 \sin \varphi \exp(-(t/\tau_2)^\gamma)]^2} \quad (2)$$

The corresponding fit is shown in Fig. 4 as a solid line. For $\gamma = 1$ a convincing fit to the measured data is impossible. The best coincidence is found with the fit parameters $\Delta n_c = 7.0 \times 10^{-5}$, $\Delta n_b^0 = 9.3 \times 10^{-5}$, $\varphi = 12.4^\circ$, $\tau_2 = 37.7$ h and $\gamma = 0.53$. The values for Δn and the angle φ agree fairly well with those found for the development process.

4 Origin of the two gratings

The time evolution of the grating Δn_b can be well explained as that of a photovoltaic grating. In LiNbO₃ crystals the photovoltaic effect is the main charge-driving force. During the fixing process a deep modulation of the Cu⁺ traps arises because the space-charge field is permanently compensated by screening ions that are mobile at high temperatures [4]. After cooling down the homogeneous illumination generates modulated photocurrents resulting from the deep modulation of the Cu⁺ traps. Now a space-charge field builds up that modulates the refractive index via the electrooptic effect and the grating Δn_b appears.

After the development process the photovoltaic grating Δn_b is slowly erased via the dark conductivity of the material. Recently, the dark erasure of holograms recorded in LiNbO₃:Fe at room temperature has been found to follow a stretched exponential function [16]. This is the type of function we use for our model to describe the dark compensation.

The permanent grating Δn_c is most likely attributed to the copper ions in the samples. This conclusion is based on the fact that the measured permanent gratings Δn_c are uniquely found in LiNbO₃:Cu and not in LiNbO₃:Fe crystals. If the grating Δn_c were formed by a deep modulation of the protons during the fixing process it should also be present in LiNbO₃:Fe, which is not the case. There are two possibilities for the copper ions to generate the grating Δn_c . First, the deep modulation of Cu⁺ and Cu²⁺ can already lead to material changes that cause a measurable sinusoidal refractive-index change in the samples. If enough ions are present for charge compensation, the modulation degree of Cu⁺ can reach almost one. Furthermore, it is not established that protons, like in LiNbO₃:Fe, are responsible for the compensation of the space-charge field during thermal fixing in LiNbO₃:Cu. The diffusion constant of copper in LiNbO₃ at 1000 °C is more than 500 times higher than that of iron under the same conditions. In our experiments the grating period is only around 350 nm. Therefore, the distance the compensating ions have to move is small. If one takes into account that during thermal fixing the ions also drift in a strong space-charge field it may be possible that the Cu²⁺ ions themselves, and not only the protons, act as compensating ions. This means that the copper concentration itself will be modulated during fixing, not only the distribution of the Cu⁺ and the Cu²⁺ ions.

We can rule out that Δn_c results from an absorption grating formed during the recording process. Cu²⁺ introduces an absorption band around 1100 nm in LiNbO₃ [2] and it may be argued that an absorption grating is generated. The absolute diffraction efficiency η_{abs} of a reflection grating of this kind, taking into account absorption losses in the sample, is limited to 7.2% [10]. Here η_{abs} is defined as the ratio I_d/I_r , where I_d is the intensity of the diffracted beam and I_r the intensity of the readout beam impinging on the sample. From a measurement with an undeveloped reflection grating thermally fixed for 140 min in the sample T4 we find a far higher value of $\eta_{\text{abs}} = 55 \pm 10\%$.

Now we discuss the phase shift between the two gratings. During homogeneous illumination electrons are excited from Cu⁺ ions into the conduction band. In doped LiNbO₃ the drift length for electrons is small. Therefore the charge distribution ρ originating from retrapped electrons has a phase shift of 90° to the Cu⁺ distribution. The resulting space-charge

field is deduced from Maxwell's relation $\text{div } \mathbf{E} = \rho / \epsilon \epsilon_0$. This introduces again a phase shift of 90° for the developed space-charge field and consequently for the grating Δn_b . This means that Δn_b and the Cu^+ distribution have a phase shift of 180° .

If the grating Δn_c results from material changes caused by a redistribution of the copper ions it will be in phase or counter-phase to the Cu^+ distribution. If we assume it to be in phase this fits our model very well. This means that Δn_b and Δn_c have a phase shift of 180° , equivalent to $\varphi = 0$ in our model. From the measurement we find that the angle φ is not exactly zero. This may be understood if we take into account that for the small grating periods around 350 nm a diffusion grating may not in any case be neglected versus the photovoltaic grating. From the relations $E_{\text{diff}} = k_B T K / e$ [17, 18] and $\Delta n_{\text{diff}} = -0.5 n^3 r E_{\text{diff}}$ we calculate a maximum strength of $\Delta n_{\text{diff}} = 1.7 \times 10^{-5}$ for the diffusion grating. Here T is the temperature, $K = 2\pi / \Lambda$ the spatial frequency, n the refractive index and r the appropriate element of the electrooptic tensor. In LiNbO_3 the diffusion and the photovoltaic gratings have a phase shift of 90° [17, 18]. Thus, if Δn_{diff} participates in Δn_b , it induces the small phase shift $\varphi \neq 0$.

5 Summary

In summary, we have reported on the formation of permanent reflection gratings in photorefractive $\text{LiNbO}_3:\text{Ti}:\text{Cu}$ channel waveguides by high-temperature recording. Strong refractive-index modulations, most likely not originating from the photorefractive effect, but from material changes, arise without the need of any development process of the gratings. Such gratings show no measurable decrease of their diffraction

efficiencies for at least one year. The maximum obtained refractive-index modulations may be further enhanced by a higher copper-doping level.

Acknowledgements. Financial support of the Deutsche Forschungsgemeinschaft (grant SFB 225, D9) is gratefully acknowledged.

References

1. A. Ashkin, G.D. Boyd, J.M. Dziedzic, R.G. Smith, A.A. Ballman, J.J. Levinstein, K. Nassau: *Appl. Phys. Lett.* **9**, 72 (1966)
2. E. Krätzig, R. Orłowski: *Ferroelectrics* **27**, 241 (1980)
3. J.J. Amodei, D.L. Staebler: *Appl. Phys. Lett.* **18**, 540 (1971)
4. K. Buse, S. Breer, K. Peithmann, S. Kapphan, M. Gao, E. Krätzig: *Phys. Rev. B* **56**, 1225 (1997)
5. V. Leyva, G.A. Rakuljic, B. O'Conner: *Appl. Phys. Lett.* **65**, 1079 (1994)
6. R. Müller, M.T. Santos, L. Arizmendi, J.M. Cabrera: *J. Phys. D: Appl. Phys.* **27**, 241 (1994)
7. C. Becker, A. Greiner, T. Oesselke, A. Pape, W. Sohler, H. Suche: *Opt. Lett.* **23**, 1194 (1998)
8. J. Hukriede, D. Kip, E. Krätzig: *J. Opt. A: Pure Appl. Opt.* **2**, 481 (2000)
9. K. Peithmann, J. Hukriede, K. Buse, E. Krätzig: *Phys. Rev. B* **61**, 4615 (2000)
10. H. Kogelnik: *Bell Syst. Tech. J.* **48**, 2909 (1969)
11. J. Hukriede, B. Gather, D. Kip, E. Krätzig: *Phys. Status Solidi A* **172**, R3 (1999)
12. A.A. Freschi, J. Frejlich: *Opt. Lett.* **20**, 635 (1995)
13. P. Hertel, K.H. Ringhofer, R. Sommerfeldt: *Phys. Status Solidi A* **104**, 855 (1987)
14. M. Carrascosa, F. Agullo-Lopez: *J. Opt. Soc. Am. B* **7**, 2317 (1990)
15. A. Yariv, S. Orlov: *Opt. Lett.* **20**, 1334 (1995)
16. I. Nee, M. Müller, K. Buse, E. Krätzig: *J. Appl. Phys.* **88**, 4282 (2000)
17. N.V. Kukhtarev: *Sov. Tech. Phys. Lett.* **2**, 438 (1976)
18. N.V. Kukhtarev, V.B. Markov, S.G. Odoulov, M.S. Soskin, V.L. Vinetskii: *Ferroelectrics* **22**, 949 (1979)